



Evolution of orbital angular momentum in a soft quasi-periodic structure with topological defects

WANG ZHANG,¹ JIE TANG,¹ PENG CHEN,¹ GUOXIN CUI,¹ YANG MING,^{1,2,3}
WEI HU,¹ AND YANQING LU^{1,4}

¹National Laboratory of Solid State Microstructures, College of Engineering and Applied Sciences, Collaborative Innovation Centre of Advanced Microstructures, Nanjing University, Nanjing 210093, China

²School of Physics and Electronic Engineering, Changshu Institute of Technology, Suzhou 215000, China

³njumingyang@gmail.com

⁴yqlu@nju.edu.cn

Abstract: A continuously deformative space possesses trivial or nontrivial topological characteristics depending on the associated homotopy groups associated with spaces describing the physical processes. Moreover, the interaction of spatial warping and structural symmetry always presents fantastic phenomena, especially in the systems with unique symmetrical properties such as quasicrystals. Here, we propose a quasi-periodic structure (QPS) with topological defects. The analytical expression of the corresponding Fourier spectrum is derived, which reflects the combined effects of topological structure and quasi-translational symmetry. Light-matter interaction therein brings unusual diffraction characteristics with exotic evolution of orbital angular momentum (OAM). Long-range correlation of QPS resulted in multi-fractal and pairwise distribution of optical singularities. A general conservation law of OAM is revealed. A liquid crystal photopatterned QPS is fabricated to demonstrate the above characteristics. Dynamic reconfigurable manipulation of optical singularities is achieved. Our approach offers the opportunity to manipulate OAM with multiple degrees of freedom, which has promising applications in multi-channel quantum information processing and high-dimensional quantum state generation.

© 2019 Optical Society of America under the terms of the [OSA Open Access Publishing Agreement](#)

1. Introduction

Topological features characterizing the global connection of a structure directly determine its physical properties. In past decades, many effects caused by variations in topological features, such as topological insulators [1,2] and the quantum Hall effect [3,4], have been observed. The topology of a structure can be changed by introducing a topological defect [5]. Such endowed global topology gives the structure the ability to reshape the wavefront of incident light to achieve orbital angular momentum (OAM) transition.

The light beam carrying quantized OAM is known as the optical singularity [6–8]. It has a singular topological phase distribution characterized by a phase winding factor $e^{il\theta}$. It has a donut-like intensity distribution that results from a phase singularity at the center of the optical axis. Owing to its unique topology, the optical singularity has quite important physical significance and practical applications, including micro-particle manipulation [9] and quantum information processing [10]. Many advances have been made in our understanding of the mechanisms of interaction for optical singularities with topologically modulated structures, both in linear [11–13] and nonlinear systems [14]. Programmable lattices of optical singularities with arbitrary distribution in space are realized [15]. However, different from our work, the focus of this work is to create spatially distributed vortex on each lattice site.

Compared to ordinary periodic structures, QPS are deterministic disordered structures with long-range order [16–18]; they can be recognized as the intermediate state between periodic structures and completely disordered structures [19,20]. The transition from periodic structure to quasi-periodic structure undergoes the breaking of translational symmetry. This means that the conservation law of linear momentum must inevitably change during the transition according to Noether's theorem [21]; it is important to recognize and understand the effect of translational symmetry on diffraction characteristics. In addition, QPS have high-dimensional complexity, which may allow for OAM manipulation with multiple degrees of freedom; that is, lots of paths to distribute, adjustable polarizations via liquid crystal and modulated nonlinear crystals combined with frequency conversion. Therefore, there is a need to study the mechanism of the interaction between optical singularities and topologically modulated QPS, both in terms of physical meaning and practical application.

In this article, we propose a one dimensional (1D) QPS with topological defects, coupling spatial warping and quasi-translational symmetry. Such structures are implemented using a soft reconfigurable liquid crystal (LC) consisting of alternative orthogonally planar aligned region, which were fabricated through photopatterning of a polarization-sensitive alignment agent with a dynamic microlithography system. The observed diffracted light field exhibited a non-aliased optical singularity distribution with multifractal features, following the formulated conservation law of OAM. Breaking the translational symmetry, we then observed the hybridization of optical singularities in 1D compound periodic structures (CPS). Further, the transformation from mixed state to pure state is revealed under the combined effects of topological defects and translational symmetry.

2. Construction scheme and principle

QPS can be obtained by the cut and project method [22,23]; that is, a restricted projection of a high-dimensional space (hyperspace) into a low-dimensional space. Therefore, the rank of the Fourier module of QPS equals the spatial dimension of the hyperspace. As a result, QPS have higher complexity than periodic systems. Accordingly, we constructed a 1D QPS as the 1D projection of a related two dimensional (2D) periodic lattice [19] and then modulated it with topological defects:

$$g(x, \phi) = \text{sign} \left\{ \cos \left(\frac{2\pi}{\Lambda} x + l_1 \phi \right) + \cos \left(\frac{2\pi\tau}{\Lambda} x + l_2 \phi \right) \right\}, \quad (1)$$

where the slope of the projection axis τ is an irrational number, and Λ is the pitch of the 2D periodic lattice. Moreover, such a structure is also considered as the incommensurately modulated structure with deterministic disorder derived from the irrational number. When the slope of the projection axis τ is a rational number, 1D compound periodic structure with periodic order is obtained based on the projection mechanism. That indicates that τ is somewhat connected with the order parameter of the structure, and we can use each certain value of τ to calibrate a 1D deterministic disordered or periodic ordered structure.

In this work, the irrational golden ratio $(1+\sqrt{5})/2$ was chosen to construct the QPS without loss of generality. The l_1 and l_2 are topological charges that can have an integer or fractional value corresponding to different topological defects, and ϕ is the azimuthal angle. This topological modulation edits the global topology of the structure and endows it with quasi-angular-momentum at the same time; this has a unique effect on diffraction characteristics. Figure 1(a) shows the structure of the QPS when the values of l_1 and l_2 are both taken as 1.

When light is diffracted by the 1D QPS with topological defects, its phase will be singularly modulated [24]. That means the incident light undergoes an OAM transition during the interaction. The distribution of the diffracted light field directly depends on the reciprocal

lattice vector structure. Therefore, in order to analyze the mechanism of interaction, it is necessary to calculate the corresponding Fourier spectrum. This calculation process is cumbersome. However, we can derive it step by step. To greatly simplify the derivation, a mathematical trick that transforms the sum of cosine to the product of cosine is need. Then we can use the properties of the Fourier transform and do some corresponding variable substitutions. The final result is given in the following expression:

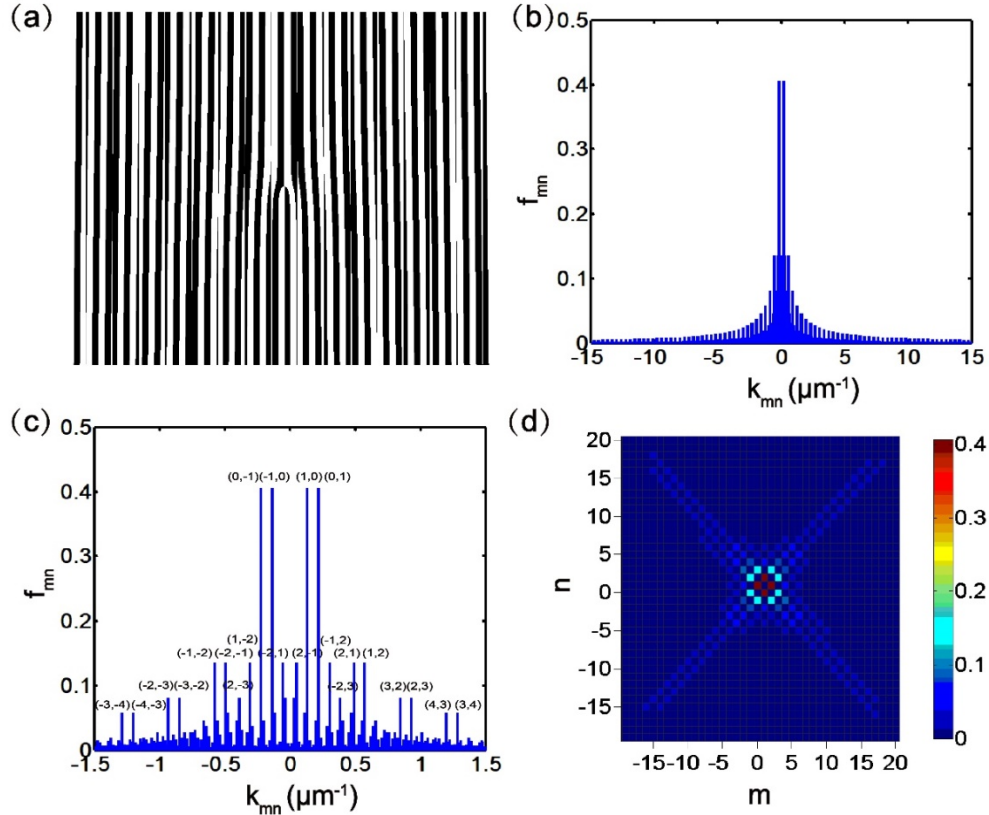


Fig. 1. Structure and Fourier spectra for QPS with $\tau = (1 + \sqrt{5})/2$ and $l_1 = l_2 = 1$. (a) Structure of the QPS; (b) Self-similar Fourier spectrum of QPS for $\max(k_{mn}) = 15 \mu\text{m}^{-1}$; (c) Fourier spectrum of the low-order diffraction part, with some diffraction orders labeled; (d) Two-dimensional distribution of the Fourier spectrum; the magnitude of the Fourier coefficient is represented by a color bar.

$$\begin{aligned} \mathcal{F}_x \{g(x, \phi)\} &= \sum_{m,n} \sin c\left(\frac{m+n}{2}\right) \sin c\left(\frac{n-m}{2}\right) e^{i(ml_1 + nl_2)\phi} \delta\left(k - \frac{2\pi}{\Lambda}(m + n\tau)\right) \\ &= \sum_{m,n} f_{mn} e^{il_{mn}\phi} \delta(k - k_{mn}), \end{aligned} \quad (2)$$

where $\sin c(x) = \sin(\pi x) / (\pi x)$, $k_{mn} = 2\pi(m + n\tau) / \Lambda$ is the reciprocal lattice vector corresponding to the diffraction order (m, n) , $l_{mn} = ml_1 + nl_2$ is the topological charge, and $f_{mn} = \sin c[(m+n)/2] \sin c[(n-m)/2]$ is the Fourier coefficient. Two indicators, m and n , are needed to calibrate the diffracted light field for our 1D QPS, which is completely different from 1D periodic structures that have only one indicator. This allowed our QPS to achieve high-dimensional manipulation of optical singularities.

3. Self-similar spectrum and multifractal analysis

According to Fraunhofer diffraction theory, the intensity of far-field diffracted light is proportional to the square of the Fourier coefficient. Figure 1(b) shows the Fourier spectrum when k_{mn} is less than $15 \mu\text{m}^{-1}$. Intuitively, the spectrum is self-similar, which is due to the long-range correlation of the structure [17,25]. This unique scaling feature can be analyzed by the so-called multifractal theory [26], which is usually used to characterize the statistical nature of a positive measure [27–29]. A positive measure is defined to describe a positive quantity that is distributed on the support of the measure. For our diffraction spectrum, the support was the reciprocal space and the positive quantity corresponded to Fourier intensity. To reveal the multifractal characteristics of the diffracted light field, the generalized dimension D_q and associated singular spectrum $f(\alpha)$ were calculated according to the approximate scheme [28]. The value of D_q corresponds to scaling exponents for q -th moments of the measure; $f(\alpha)$ is the dimension of the relative strength. The results are shown in Fig. 2.

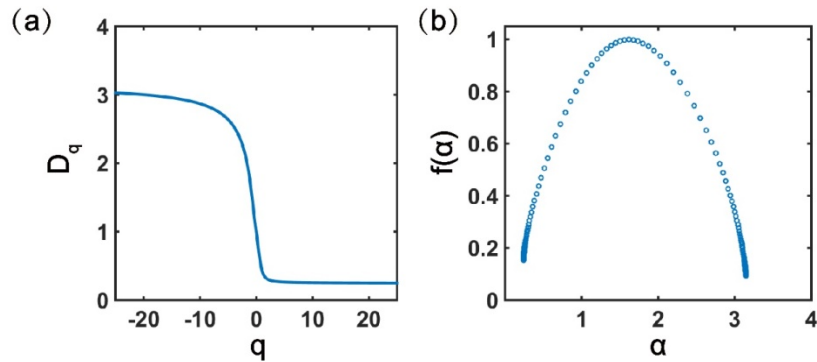


Fig. 2. Multifractal analysis of the Fourier spectrum for QPS. (a) Generalized dimension D_q ; (b) Associated singular spectrum $f(\alpha)$. Maximum values of the Fourier coefficient subscript m (or n) and the order q for numerical calculation are 40 and 50, respectively.

The most rarefied and the most concentrated regions of the intensity measure were characterized by $\alpha_{\max} = \lim_{q \rightarrow -\infty} D_q$ and $\alpha_{\min} = \lim_{q \rightarrow +\infty} D_q$, respectively. The dimensions of $D_0 = f(\alpha_0) = 1$ arise from the whole real k_{mn} . The numerically calculated $f(\alpha)$ curve exhibited perfect smoothness, as shown in Fig. 2(b), which is the feature of an infinite structure. In Fig. 2(a), one can easily find the information dimension $D_1 < D_0$, which indicates that the intensity distribution of the diffracted optical singularities is a fractal measure.

4. Interaction between OAM and QPS

It is noteworthy that optical singularities are characterized by the carried OAM [6]. Therefore the evolution of optical singularities directly corresponds to the numerical variation in OAM. In the interaction between the optical singularity and the proposed structure, the distribution of pure optical singularities with non-degenerate OAM was observed, as shown in Fig. 3. Following the conservation of angular momentum, we identified a general conservation law of OAM in this system.

Firstly, we verified the non-degenerate nature of the reciprocal lattice vector structure of the QPS. Suppose that two diffraction orders, (m, n) and (m', n') , are degenerate with each other, k_{mn} must equal to $k_{m'n'}$. The slope of the projection axis can then be expressed by the form of a fractional number $\tau = (m' - m) / (n - n')$, which is contrary to the construction

mechanism; therefore, for a QPS, it has a non-degenerate diffraction field distribution. That is, for any diffraction order, optical singularities carry only a single OAM value. That value is naturally derived from Eq. (2), expressed as:

$$l_{mn} = ml_1 + nl_2. \quad (3)$$

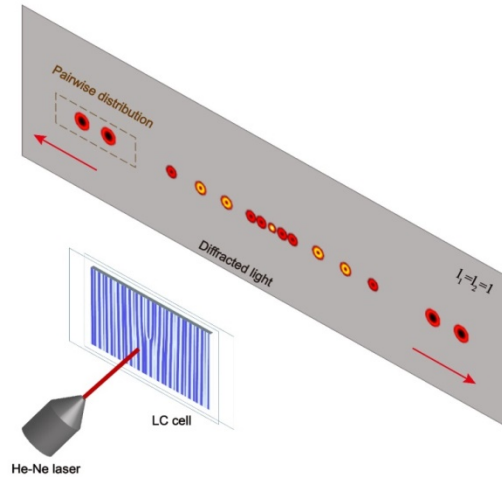


Fig. 3. Schematic illustration of experiment. A Gaussian beam emitted by a He-Ne laser incident on a reconfigurable photo-patterned liquid crystal (LC) cell. Optical singularities carrying OAM are generated and detected. Here we show the result of topological defects modulated with a QPS of $l_1 = l_2 = 1$.

Equation (3) indicates the conservation law of OAM in a QPS with topological defects. Considering the whole process, the input photons interacting with a topological defects modulated structure are imprinted with the structure's topological charges in order to conserve the total angular momentum. Therefore, Eq. (3) also indicates the conservation law of OAM in a QPS with topological defects. The theoretical and experimental results of QPS with different topological defects are shown in Fig. 4. The diffraction orders were calibrated according to Fig. 1(c), and the corresponding OAM distribution was constrained to the conservation law. The optical singularities of any diffraction order carried a single OAM, as expected; these were regarded as pure states. The experimental results were in good agreement with theoretical simulations. Furthermore, it is noteworthy that the distribution of optical singularities is pairwise. Dotted rectangular frames in Fig. 4 mark two diffraction points' pairs at low order diffraction; the paired diffraction orders are:

$$(m, m-1) \text{ and } (m-1, m), \quad (4)$$

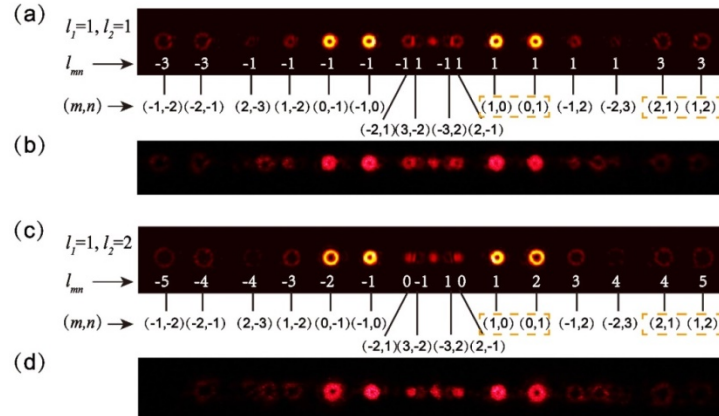


Fig. 4. Experimental and numerical distributions of diffracted optical singularities in QPS with various topological defects. The golden ratio $(1 + \sqrt{5}) / 2$ is picked as the irrational number in all QPS. (a, b) Numerical and experimental results for $l_1 = l_2 = 1$; (c, d) Numerical and experimental results for $l_1 = 1$ and $l_2 = 2$. Diffraction orders (m, n) are labeled by brackets with two indices; the carried OAM of optical singularities are indicated correspondingly.

Such an effect is directly derived from the characteristics of the pairwise distribution of the Fourier spectrum. The Fourier coefficient f_{mn} is in the form of the product of two sinc functions, as expressed in Eq. (2). Thus, the non-zero component in the spectrum must satisfy $m + n = \text{odd}$ and $n - m = \text{odd}$ at the same time. Based on this, diffraction orders corresponding to the larger intensity should satisfy $n - m = \pm 1$ or $m + n = \pm 1$. For the condition of $n - m = \pm 1$, it gives the result of paired diffraction orders which are not only immediately adjacent but also close in intensity just expressed by Eq. (4). And for the condition of $m + n = \pm 1$, the given paired diffraction orders are separated on both sides of the spectrum and the intensities of most of them are too low to be recognized. Therefore, we mainly focus on the former pairwise distribution in this work. This feature can be understood more intuitively from the Fourier spectrum shown in Fig. 1(d). For example, when m and n are both greater than 10, the pairwise distribution defined by the diffraction order above can be clearly seen.

5. Compared CPS and optical singularities transformation

The 1D CPS is proposed to reveal the combined effects of topological structure and quasi-translational symmetry on diffraction characteristics and the evolution of OAM. In general, 1D CPS can be constructed in a way similar to the projection method; however, unlike the QPS, the slope of the projection axis here is a rational number instead. According to previous analysis, the reciprocal lattice vector structure of CPS must be degenerate. That means for any diffraction spot, it is actually composed of an infinite number of diffraction orders. If diffraction order (m, n) and (m', n') are degenerate with each other, we can get the equation $k_{mn} = k_{m'n'}$ which can be easily expressed as $m + n\tau = m' + n'\tau$. The slope γ corresponding to the degenerate axis on the Fourier spectrum is directly derived from that equation.

$$\gamma = \frac{n' - n}{m' - m} = -\frac{1}{\tau}, \tag{5}$$

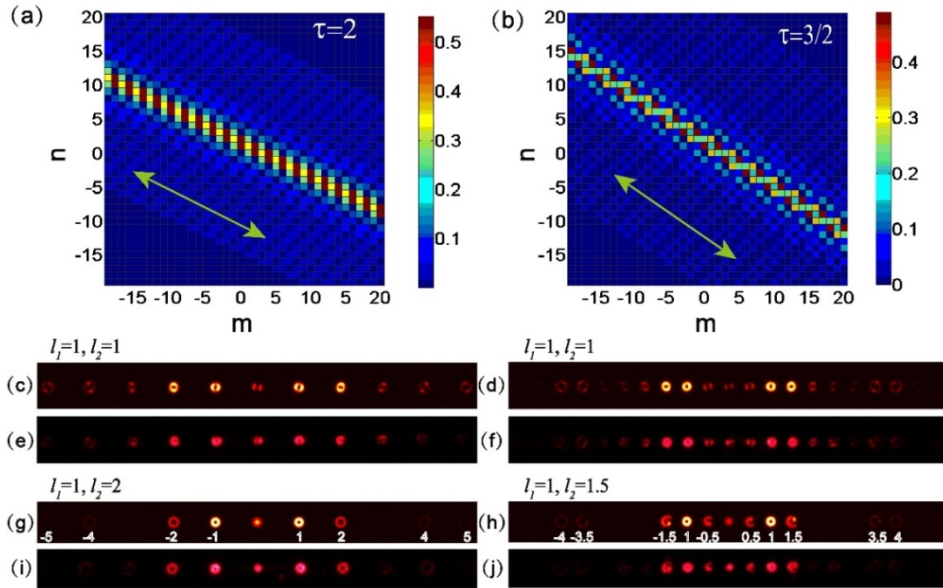


Fig. 5. Experimental and numerical distributions of diffracted optical singularities in CPS with various topological defects. (a, b) Fourier spectra for various CPS with $\tau = 2$ and $\tau = 3/2$, respectively; the degenerate axis is indicated by a green arrow; (c, e) Numerical and experimental results for an arbitrary topological defects doping case in CPS with $\tau = 2$; (g, i) Numerical and experimental results under the specific condition $l_2 = \tau l_1$ in CPS with $\tau = 2$; (d, f, h, j) Analogy results of CPS with $\tau = 3/2$.

Figures 5(a) and 5(b) show the Fourier coefficient spectra of the CPS with $\tau = 2$ and $\tau = 3/2$, respectively. The slopes of their degenerate axes are $-1/2$ and $-2/3$, as indicated by the green arrow, which is in full agreement with the theoretical analyses. One can imagine that topological charge corresponding to the degenerate reciprocal lattice vector structure should also be degenerate under ordinary circumstances. That means, a mixed state with the hybrid optical singularity diffraction distribution shown in Figs. 5(c)-5(f) will be observed under the transition of translational symmetry. However, when the structure parameters satisfy $l_2 = \tau l_1$, the transformation from the mixed state into the pure state was observed as shown in Figs. 5(g)-5(j). The reason for this special phenomenon is that optical singularities degenerated at the same diffracted spot carry the same value of OAM under such a condition. The transition of optical singularities demonstrates the combined effects of topological structure and translational symmetry.

6. LC photopatterning and experimental setup

The photo alignment technique is a suitable way to achieve high-resolution patterned domain LC alignments [30]. The designed LC orientations were performed through computer-controlled photopatterning via a dynamic microlithography system [12]. Here, we choose sulphonic azo-dye SD1 (DIC, Japan) as the alignment agent owing to its polarization-sensitive and rewritable advantages. LC directors are guided by the absorption oscillators of SD1 molecules, which are perpendicular to the incident UV light polarization [31]. Two pieces of glass substrates coated with SD1 were assembled to form a $6.0\text{-}\mu\text{m}$ thickness cell. Afterwards, we took a two-step photo exposure to achieve the adjacent orthogonal planar aligned regions in order to avoid the influence of polarization sensitivity [11]. Finally, the designed structures were obtained by filling the cell with LC E7.

A linearly polarized 632.8-nm He-Ne laser illuminated the LC cell normally, as shown in Fig. 3(a) digital CCD camera was used to capture the diffraction patterns. The value of pitch Λ in our experiment is 46.3 μm . Figure 4 shows the experimental results (Figs. 4(b) and 4(d)) and the compared numerical simulations (Figs. 4(a) and 4(c)) with different topological defects modulating QPS. The distribution of the diffracted optical singularities and the corresponding OAM are indicated clearly. In all cases, the obtained optical singularities were completely pure owing to the single carried OAM. This confirms the QPS can achieve high-dimensional modulation of optical singularities. In Fig. 5(a), Fourier spectra for CPS with $\tau = 2$ are given. They have a degenerate axis with the slope $\gamma = -1/\tau$, as indicated by the green arrow. The corresponding experimental and theoretical results are shown in Figs. 5(e) and 5(i) and Figs. 5(c) and 5(g), respectively. The right column in Fig. 5 shows the juxtaposed results for CPS with $\tau = 3/2$. Figs. 5(c)-5(f) show that the diffracted optical singularities were all hybrid for an arbitrary modulated case, reflecting the transition of translational symmetry. However, when the structure parameters satisfied $l_2 = \tau l_1$, the mixed optical singularities were transformed into pure ones, as shown in Figs. 5(g)-5(j), reflecting the combined modulation of topological structure and translational symmetry. It's necessary to note that there is light leakage in order zero due to the accuracy of the structure fabrication shown in Fig. 1(a). With a higher precision fabrication method, the light leakage can be completely suppressed. In our numerical simulation, we re-normalized the intensity of the diffracted light field by considering the reduced conversion efficiency due to the light leakage.

7. Discussions and conclusions

We have mainly presented results for when the light beam carrying $l_0 = 0$ OAM was normally incident on the center of the structure. We also experimentally tested the case of $l_0 \neq 0$. The conservation law of OAM was then expressed as a generalized form: $l_{mn} = l_0 + ml_1 + nl_2$. When the incident position of the optical singularity did not coincide with the topological dislocation of the structure, coupling of spin and orbital angular momentum was taken into consideration. The evolution of OAM under such conditions was not intuitive and requires further investigation. Furthermore, other structured beams also deserve to be studied in this topological modulated QPS.

We choose LC as our experimental platform owing to its excellent electro-optical and soft reconfigurable properties. Based on photopatterning technology, LC offers the possibility to fabricate complex geometric phase structures. Yet, it is essentially a linear system. Correspondingly, a potential extension to our work would be to investigate the interaction of an optical singularity with QPS or CPS in a nonlinear system such as a LiNbO_3 crystal. Owing to the mix of OAM and frequency, more abundant unprecedented physical features can be shown. For example, novel entanglement with multiple superposition of OAM eigenstates can be obtained by turning the structural parameters based on spontaneous parametric down conversion [32].

Furthermore, a simple 1D QPS with 2D complexity is proposed here. Higher dimensional information can be compressed to 1D to construct a QPS according to our method. Moreover, the spatial dimension of the structure can also be extended to 2D and 3D. This may provide the possibility to achieve high dimensional and multi-degree-of-freedom regulation for OAM. Thus, such a system can theoretically achieve more parallel detection of OAM states than before. In addition, it may be used to verify violations of Bell-type inequalities of high-dimensional systems [33]. Considering a specific application, the high-dimensional complexity gives out more paths for the input OAM to be distributed. As for different paths are encoded with different OAMs according to the conservation law, this path-OAM coupling provides the possibility to switch OAM entanglement to path entanglement [34].

In conclusion, we proposed a 1D quasi-periodic structure with topological defects to reveal the effects of topological defects and translational symmetry on the evolution of orbital angular momentum. The structural parameters were flexible owing to the soft reconfigurable liquid crystal constructed using photopatterning technology. A general conservation law of orbital angular momentum was revealed. We observed the distribution of diffracted optical singularities, which exhibited multifractal and pairwise features. We found that the transition of translational symmetry can lead to the hybridization of optical singularities. The transformation from mixed state to pure state under $l_2 = \tau l_1$ was observed, which demonstrates the combined effects of topological structure and translational symmetry. Furthermore, these proposed structures with high-dimension complexity can manipulate orbital angular momentum with multiple degrees of freedom, which is promising for multi-channel quantum information processing and high-dimensional quantum state generation.

Funding

National Key R&D Program of China (2017YFA0303700), National Natural Science Foundation of China (NSFC) (61490714, 11704182, and 11604144), Fundamental Research Funds for the Central Universities (14380001).

Acknowledgments

We thank Prof. Chao Zhang, Li-Jian Zhang and Li-Xiang Chen for helpful discussions.

References

1. M. Z. Hasan and C. L. Kane, "Colloquium: Topological insulators," *Rev. Mod. Phys.* **82**(4), 3045–3067 (2010).
2. L. Lu, J. D. Joannopoulos, and M. Soljačić, "Topological photonics," *Nat. Photonics* **8**(11), 821–829 (2014).
3. M. A. Levin and X.-G. Wen, "String-net condensation: A physical mechanism for topological phases," *Phys. Rev. B Condens. Matter Mater. Phys.* **71**(4), 045110 (2005).
4. L. Lu, J. D. Joannopoulos, and M. Soljačić, "Topological states in photonic systems," *Nat. Phys.* **12**(7), 626–629 (2016).
5. N. D. Mermin, "The topological theory of defects in ordered media," *Rev. Mod. Phys.* **51**(3), 591–648 (1979).
6. L. Allen, M. W. Beijersbergen, R. J. C. Spreeuw, and J. P. Woerdman, "Orbital angular momentum of light and the transformation of Laguerre-Gaussian laser modes," *Phys. Rev. A* **45**(11), 8185–8189 (1992).
7. A. T. O'Neil, I. MacVicar, L. Allen, and M. J. Padgett, "Intrinsic and extrinsic nature of the orbital angular momentum of a light beam," *Phys. Rev. Lett.* **88**(5), 053601 (2002).
8. A. M. Yao and M. J. Padgett, "Orbital angular momentum: origins, behavior and applications," *Adv. Opt. Photonics* **3**(2), 161–204 (2011).
9. L. Paterson, M. P. MacDonald, J. Arlt, W. Sibbett, P. E. Bryant, and K. Dholakia, "Controlled rotation of optically trapped microscopic particles," *Science* **292**(5518), 912–914 (2001).
10. Z.-Y. Zhou, S.-L. Liu, Y. Li, D.-S. Ding, W. Zhang, S. Shi, M.-X. Dong, B.-S. Shi, and G.-C. Guo, "Orbital angular momentum-entanglement frequency transducer," *Phys. Rev. Lett.* **117**(10), 103601 (2016).
11. P. Chen, S.-J. Ge, L.-L. Ma, W. Hu, V. Chigrinov, and Y.-Q. Lu, "Generation of equal-energy orbital angular momentum beams via photopatterned liquid crystals," *Phys. Rev. Appl.* **5**(4), 044009 (2016).
12. P. Chen, L.-L. Ma, W. Duan, J. Chen, S.-J. Ge, Z.-H. Zhu, M.-J. Tang, R. Xu, W. Gao, T. Li, W. Hu, and Y.-Q. Lu, "Digitalizing Self-Assembled Chiral Superstructures for Optical Vortex Processing," *Adv. Mater.* **30**(10), 1705865 (2018).
13. J. Kobashi, H. Yoshida, and M. Ozaki, "Polychromatic optical vortex generation from patterned cholesteric liquid crystals," *Phys. Rev. Lett.* **116**(25), 253903 (2016).
14. N. V. Bloch, K. Shemer, A. Shapira, R. Shiloh, I. Juwiler, and A. Arie, "Twisting light by nonlinear photonic crystals," *Phys. Rev. Lett.* **108**(23), 233902 (2012).
15. R. Barboza, U. Bortolozzo, G. Assanto, E. Vidal-Henriquez, M. G. Clerc, and S. Residori, "Harnessing optical vortex lattices in nematic liquid crystals," *Phys. Rev. Lett.* **111**(9), 093902 (2013).
16. D. Shechtman, I. Blech, D. Gratias, and J. W. Cahn, "Metallic phase with long-range orientational order and no translational symmetry," *Phys. Rev. Lett.* **53**(20), 1951–1953 (1984).
17. M. Kohmoto, B. Sutherland, and K. Iguchi, "Localization of optics: Quasiperiodic media," *Phys. Rev. Lett.* **58**(23), 2436–2438 (1987).
18. D. Levine and P. J. Steinhardt, "Quasicrystals: a new class of ordered structures," *Phys. Rev. Lett.* **53**(26), 2477–2480 (1984).
19. E. Maciá, "The role of aperiodic order in science and technology," *Rep. Prog. Phys.* **69**(2), 397–441 (2006).
20. S. Zhu, Y. Y. Zhu, and N. B. Ming, "Quasi-phase-matched third-harmonic generation in a quasi-periodic optical superlattice," *Science* **278**(5339), 843–846 (1997).

21. E. Noether, "Invariant variation problems," *Transp. Theory Stat. Phys.* **1**(3), 186–207 (1971).
22. T. Janssen, "Crystallography of quasi-crystals," *Acta Crystallogr. A* **42**(4), 261–271 (1986).
23. W. Steurer and D. Sutter-Widmer, "Photonic and phononic quasicrystals," *J. Phys. D* **40**(13), R229–R247 (2007).
24. V. Y. Bazhenov, M. S. Soskin, and M. V. Vasnetsov, "Screw dislocations in light wavefronts," *J. Mod. Opt.* **39**(5), 985–990 (1992).
25. W. Gellermann, M. Kohmoto, B. Sutherland, and P. C. Taylor, "Localization of light waves in Fibonacci dielectric multilayers," *Phys. Rev. Lett.* **72**(5), 633–636 (1994).
26. T. C. Halsey, M. H. Jensen, L. P. Kadanoff, I. Procaccia, and B. I. Shraiman, "Fractal measures and their singularities: The characterization of strange sets," *Phys. Rev. A Gen. Phys.* **33**(2), 1141–1151 (1986).
27. A. Chhabra and R. V. Jensen, "Direct determination of the $f(\alpha)$ singularity spectrum," *Phys. Rev. Lett.* **62**(12), 1327–1330 (1989).
28. C. Godreche and J. M. Luck, "Multifractal analysis in reciprocal space and the nature of the Fourier transform of self-similar structures," *J. Phys. A* **23**(16), 3769–3797 (1990).
29. D. Tanese, E. Gurevich, F. Baboux, T. Jacqmin, A. Lemaître, E. Galopin, I. Sagnes, A. Amo, J. Bloch, and E. Akkermans, "Fractal energy spectrum of a polariton gas in a Fibonacci quasiperiodic potential," *Phys. Rev. Lett.* **112**(14), 146404 (2014).
30. S. Martin, S. Klaus, K. Vladimir, and C. Vladimir, "Surface-induced parallel alignment of liquid crystals by linearly polymerized photopolymers," *Jpn. J. Appl. Phys.* **31**(1), 2155–2164 (1992).
31. V. Chigrinov, S. Pikin, A. Verevochnikov, V. Kozenkov, M. Khazimullin, J. Ho, D. D. Huang, and H.-S. Kwok, "Diffusion model of photoaligning in azo-dye layers," *Phys. Rev. E Stat. Nonlin. Soft Matter Phys.* **69**(6 Pt 1), 061713 (2004).
32. Y. Ming, J. Tang, Z. Chen, F. Xu, L. Zhang, and Y. Lu, "Generation of N00N state with orbital angular momentum in a twisted nonlinear photonic crystal," *IEEE J. Sel. Top. Quantum Electron.* **21**(3), 225–230 (2015).
33. A. C. Dada, J. Leach, G. S. Buller, M. J. Padgett, and E. Andersson, "Experimental high-dimensional two-photon entanglement and violations of generalized Bell inequalities," *Nat. Phys.* **7**(9), 677–680 (2011).
34. R. Fickler, R. Lapkiewicz, M. Huber, M. P. Lavery, M. J. Padgett, and A. Zeilinger, "Interface between path and orbital angular momentum entanglement for high-dimensional photonic quantum information," *Nat. Commun.* **5**(1), 4502 (2014).